The American Journal of Pathology, Vol. 183, No. 3, September 2013

The American Journal of
PATHOLOGY
ajp.amjpathol.org

CELL INJURY, REPAIR, AGING, AND APOPTOSIS

Gadolinium Contrast Agent-Induced CD163$^+$ Ferroportin$^+$ Osteogenic Cells in Nephrogenic Systemic Fibrosis

Sundararaman Swaminathan,*† Chhanda Bose,*† Sudhir V. Shah,*† Kimberly A. Hall,‡ and Kim M. Hiatt‡

From the Division of Nephrology, Department of Internal Medicine, and the Departments of Pathology and Dermatology,‡ University of Arkansas for Medical Sciences, Little Rock; and the Renal Section,† Medicine Service, Central Arkansas Veterans Healthcare System, Little Rock, Arkansas*

Accepted for publication June 5, 2013.

Address correspondence to: Sundararaman Swaminathan, M.D., Division of Nephrology, University of Virginia Health Sciences Center, PO Box 800133, Charlottesville, VA 22908-0133. E-mail: SS4SA@hscmail.mcc.virginia.edu.

Gadolinium-based contrast agents are linked to nephrogenic systemic fibrosis in patients with renal insufficiency. The pathology of nephrogenic systemic fibrosis is characterized by abnormal tissue repair: fibrosis and ectopic ossification. The mechanisms by which gadolinium could induce fibrosis and ossification are not known. We examined *in vitro* the effect of a gadolinium-based contrast agent on human peripheral blood mononuclear cells for phenotype and function relevant to the pathology of nephrogenic systemic fibrosis using immunofluorescence, flow cytometry, real-time PCR, and osteogenic assays. We also examined tissues from patients with nephrogenic systemic fibrosis, using IHC to identify the presence of cells with phenotype induced by gadolinium. Gadolinium contrast induced differentiation of human peripheral blood mononuclear cells into a unique cellular phenotype—CD163$^+$ cells expressing proteins involved in fibrosis and bone formation. These cells express fibroblast growth factor (FGF)23, osteoblast transcription factors Runt-related transcription factor 2, and osterix, and show an osteogenic phenotype in *in vitro* assays. We show *in vivo* the presence of CD163$^+$/procollagen-1$^+$/osteocalcin$^+$ cells in the fibrotic and calcified tissues of nephrogenic systemic fibrosis patients. Gadolinium contrast—induced CD163$^+$/ferroportin$^+$/FGF23$^+$ cells with osteogenic potential may play a role in systemic fibrosis and ectopic ossification in nephrogenic systemic fibrosis. *(Am J Pathol 2013, 183: 796—807; http://dx.doi.org/10.1016/j.ajpath.2013.06.008)*

Nephrogenic systemic fibrosis (NSF) is a debilitating fibrosing illness observed in patients with advanced renal insufficiency. Gadolinium-based contrast agent exposure has been associated strongly with the development of NSF.[1,2] NSF is characterized by pathologic tissue repair—fibrosis, angiogenesis,[3,4] and ectopic ossification.[5–8] The cell population in NSF is phenotypically heterogeneous,[9] and the presence of osseous metaplasia is a strong histologic predictor of NSF.[10] We recently reported that gadolinium-based contrast agents induce iron mobilization, that iron accumulates in the tissues of NSF patients,[2,11] and that NSF is associated with calciphylaxis and increased cardiac and vascular mortality.[2,5,11] CD163 and ferroportin are markers of alternatively activated macrophages. CD163 serves as an endocytic receptor for heme and ferroportin is the only known iron exporter in the body. Osteocalcin and osteopontin are bone matrix proteins expressed by cells of osteoblast lineage, and expression of these markers by circulating cells correlates with their osteogenic and mineralizing function.[12,13] The molecular and cellular mechanisms by which gadolinium-based contrast agents trigger pathologic fibrosis, ossification, and iron accumulation in NSF are currently unknown. In this article, we report novel observations that a gadolinium-based contrast agent (Omniscan; GE Healthcare, Inc., Cleveland, OH) induces CD163$^+$/ferroportin$^+$ cells with osteogenic potential *in vitro* and we identify the presence of CD163$^+$/ferroportin$^+$/procollagen-1$^+$/osteocalcin$^+$ cells in the tissues of NSF patients.

Supported by a University of Arkansas for Medical Sciences Clinical Center for Translational Research (parent grant 1 UL1R R029884) pilot study award, a KL2 award, a South Central VA Healthcare Network Research Grants Program award, and by a VA Merit Review award (S.V.S.).

S.S. and C.B. contributed equally to this work.

Current address of S.S., Division of Nephrology, University of Virginia Health Sciences Center, Charlottesville, VA.

http://dx.doi.org/10.1016/j.ajpath.2013.06.008

Materials and Methods

For *in vitro* experiments, human peripheral blood mononuclear cells (PBMCs) were obtained from Astarte Biologics (Redmond, WA). Omniscan (gadolinium−diethylenetriamine penta-acetic acid bismethylamide plus excess calcium−diethylenetriamine penta-acetic acid bismethylamide) was used as the gadolinium contrast agent because it is known to be associated with most cases of NSF.[14]

Culture and Treatment of PBMCs

The viability of PBMCs was checked by a trypan blue dye exclusion test. Cells were cultured in Dulbecco's modified Eagle's medium (DMEM) (ATCC, Manassas, VA), containing 10% heat-inactivated serum (ATCC), penicillin, streptomycin, L-glutamine (complete medium), and treated with various doses (0.1, 0.5, and 2.5 mmol/L) of Omniscan for 5 to 10 days. Omniscan (0.1, 0.5, and 2.5 mmol/L) compared with controls induced significant cell death under serum-free conditions at 24 hours; thus, our culture conditions included the addition of 10% serum. We chose these Omniscan doses based on dose-titration experiments and a cytotoxicity assay. Omniscan induced its effects on cell differentiation between 5 and 10 days, with the most significant effect observed at 8 days. Therefore, we maintained all our culture experiments for 8 days. Our controls included cells grown with culture medium alone, without Omniscan, and cells grown with 0.1 mmol and 0.5 mmol Omnipaque (an iodinated contrast not associated with NSF but with osmolality comparable with Omniscan). At the end of the experiments, cells were washed with 1× PBS and used for the following studies. Each study was repeated at least six times using PBMCs obtained from different donors. Donors were healthy males 40 to 55 years of age with diverse racial backgrounds (African American, Hispanic, and white).

Cell Viability and Cytotoxicity Assays

PBMCs were plated and treated in 96-well plates. Various concentrations of Omniscan were added, and the viability of adherent cells was measured at 8 days using a cell-counting kit (CCK-8 colorimetric assay) from Dojindo Molecular Technologies (Gaithersburg, MD). Because the absorbance at 460 nm is proportional to the number of viable cells in the medium, the viable cell number was determined using the absorbance value of a previously prepared calibration curve. The cytotoxic effect of Omniscan was evaluated by measuring the percentage of lactate dehydrogenase released by human PBMCs, which were seeded in 96-well microplates with Roswell Park Memorial Institute (RPMI-1640) medium containing 10% fetal bovine serum. Adherent cells were lysed. Supernatant media were collected from these cultures and analyzed for lactate dehydrogenase concentration using the Cytoscan Lactate Dehydrogenase Cytotoxicity Assay kit from G-Biosciences (St. Louis, MO). Cell proliferation was assessed using DAPI and Ki-67 staining.

Immunofluorescence

Total PBMCs were seeded in fibronectin-coated, 4-well BD Biocoat chamber slides (Fisher Scientific, Pittsburgh, PA) at a density of 1000×10^3 cells/chamber in Dulbecco's modified Eagle's medium containing 10% heat-inactivated serum and treated with various doses of Omniscan for 8 days. Immunofluorescence studies were performed to examine the expression of CD163, CD34, CD206, heme oxygenase-1, H-ferritin, von Willebrand factor (CD31, Ulex lectin; Sigma-Aldrich, St. Louis, MO), acetylated low-density lipoprotein, osteocalcin, osteopontin, and procollagen-1 (all from Santa Cruz Biotechnology, Inc., Santa Cruz, CA), and ferroportin and fibroblast growth factor (FGF)23 (Abcam, Cambridge, MA). After treatment, cells were washed with 1× PBS and fixed with 4% neutral buffer formaldehyde for 15 minutes at room temperature. Slides were washed with 1× PBS three times for 5 minutes each and rinsed with 100% alcohol. Nonspecific sites were blocked by incubating the cells in 0.1% Triton X-100 (Sigma-Aldrich) and 5% goat serum for 30 minutes at room temperature, and slides then were washed three times with 1× PBS for 5 minutes each. Cells were incubated with 2 to 10 μg/mL primary antibodies (described previously) and diluted in 1% bovine serum albumin and 1× PBS at 37°C for 1 hour. Cells were washed five times with 1× PBS for 5 minutes each. Fluorescein isothiocyanate (FITC) or Texas red conjugated (Santa Cruz Biotechnology, Inc.) AlexaFluor 488 and 546 anti-goat and mouse IgG (Life Technologies, Grand Island, NY) secondary antibodies (2 to 10 μg/mL) were diluted with 5% goat serum in 1× PBS and added to the cells and incubated at 37°C for 1 hour. Cells were incubated with isotype-matched nonspecific antibodies for control. Cells were washed five times with 1× PBS for 5 minutes each and mounted with Vectashield Mounting Media (Vector Laboratories, Burlingame, CA) containing DAPI for counterstaining the nuclei. Slides were observed under a fluorescence microscope (Olympus America, Melville, NY).

Western Blot Analysis

SDS-PAGE was performed in 4% to 12% Bis-Tris NuPAGE separating gel (Life Technologies). Equal amounts of protein were loaded into each lane, and the fractionated protein was electroblotted onto nitrocellulose membranes at 30 V for 1 hour at room temperature. Membranes were blocked in casein blocker (Pierce Biotechnology, Rockford, IL) for 1 hour at room temperature and then probed with primary antibodies (anti-CD163, anti-CD206, anti-osteocalcin, anti-osteopontin, anti−procollagen-1, anti-ferroportin, anti−H-ferritin, anti−heme oxygenase-1 (all from Santa Cruz Biotechnology, Inc.), anti−Tie-2 (R&D Systems, Inc., Minneapolis, MN), and anti-CD31, anti-CD131, and anti-FGF23 (Abcam)

(diluted to 1:1000 in casein blocker), and incubated overnight at 4°C using gentle shaking. Membranes were washed five times (5 minutes each) with Tris-buffered saline with the detergent Tween-20 [TBST; 20 mmol/L Tris•HCl (pH 7.6), 137 mmol/L NaCl, and 0.2% (vol/vol) Tween 20], and incubated with horseradish-peroxidase–coupled anti-IgG (secondary antibody, dilution 1:2000) for 1 hour at room temperature. Enhanced chemiluminescence (ECL+; Amersham Biosciences, Piscataway, NJ) and fluorescence detection steps were followed for visualization of the bands. Bands were quantified using a ChemiImager 5500 (α Innotech, Corp., San Leandro, CA).

Flow Cytometry

After culture of PBMCs and treatment with gadolinium contrast for the required time period as described earlier, cells were analyzed for expression of various markers by flow cytometry. In brief, cells were harvested either by incubating with trypsin EDTA solution for 5 minutes or by gentle scratching with a cell scraper after 30 minutes of incubation on ice and washed with cold 1× PBS. After blocking Fc-receptors with 1 μg/mL human IgG (Sigma-Aldrich) for 20 minutes, samples were centrifuged at 200 × *g* for 5 minutes. Cells were washed with cold 1× cold PBS. Cell samples (0.5×10^6 to 1×10^6 cells) were incubated on ice with sample blocking buffer (10% mouse/goat serum + 1% bovine serum albumin) to block nonspecific sites. After 20 minutes of incubation, samples were centrifuged at 200 × *g* for 5 minutes. Cells were stained with either unconjugated or phycoerythrin/FITC- or allophycocynin-conjugated mouse or goat antibodies for CD163 (eBiosciences, Inc., San Diego, CA), ferroportin, CD31, CD34, von Willebrand factor, heme oxygenase-1, Tie-2 (R&D Systems, Inc.), procollagen-1, osteocalcin (R&D Systems, Inc.), osteopontin, FGF23 (Santa Cruz Biotechnology, Inc.), and CD206 (Santa Cruz Biotechnology, Inc.), 0.25 μg in 100 μL total volume of cell-staining buffer (eBiosciences, Inc.), and incubated for 45 minutes on ice in the dark. Cell samples were washed two times in 2 mL of staining buffer at 200 × *g* for 5 minutes in cold buffer. For unconjugated antibody (CD206, procollagen-1, and FGF23), after washings, cells were incubated with FITC-conjugated goat anti-mouse IgG (Santa Cruz Biotechnology, Inc.) or FITC-conjugated donkey anti-goat IgG for 45 minutes on ice in the dark. For intracellular staining, cells were fixed in cold 4% paraformaldehyde and permeabilized in cell permeabilization buffer (Santa Cruz Biotechnology, Inc.). For control, cells were incubated with the same amount of

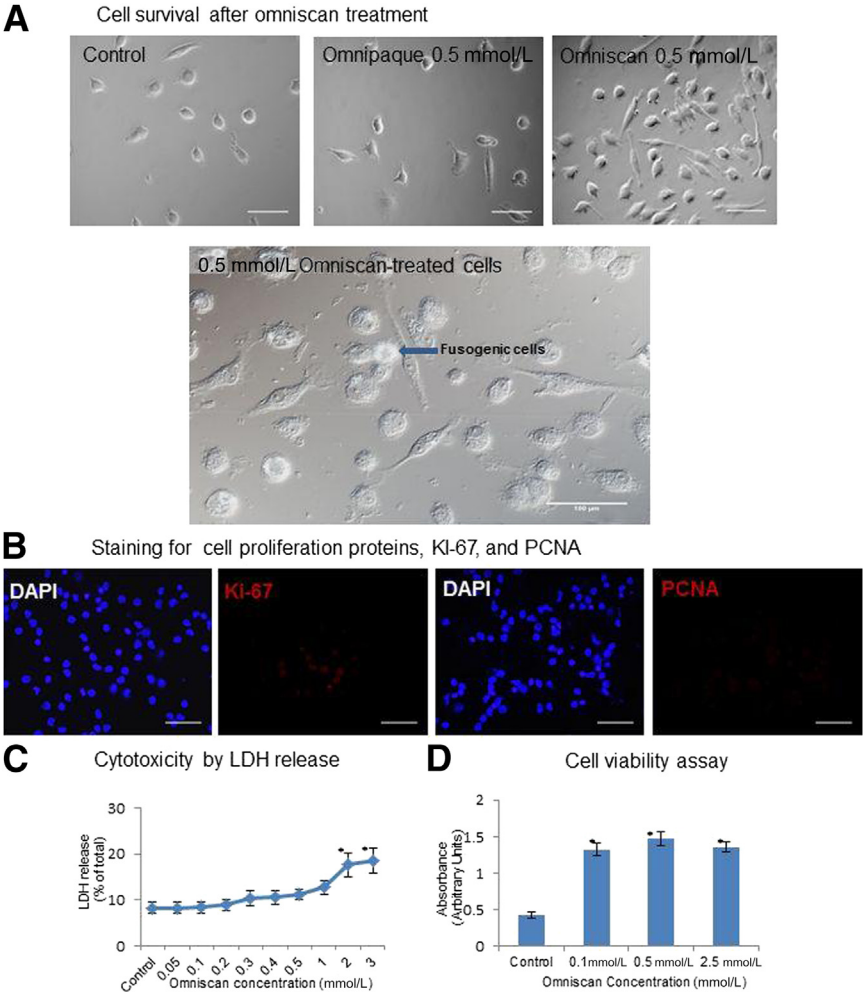

Figure 1 Omniscan induces differentiation of PBMCs into adherent cells *in vitro*. Human PBMCs were cultured with and without 0.5 mmol gadolinium contrast (Omniscan) for 8 days. **A**: Effect of Omniscan on cell differentiation. Omniscan induced *in vitro* differentiation of human PBMCs into adherent spindled cells by day 8, compared with PBMCs cultured without Omniscan (control; 0.5-mmol Omnipaque). In addition to being spindled, Omniscan-treated cells were also plump in appearance and some cells were fused together (**lower panel**). Original magnification, ×40. Scale bar = 100 μm. **B**: Effect of Omniscan on cell proliferation. DAPI staining showed an increased number of nuclei in Omniscan-treated cells compared with controls. No nuclear division was present. Ki-67/proliferating cell nuclear antigen (PCNA) (red) staining showed only the background stain, indicating a lack of cell proliferation. **C**: Effect of Omniscan on cell cytotoxicity. Adherent cells were lysed; supernatant media were collected from these cultures and analyzed for released lactate dehydrogenase (LDH). The data show no significant cytotoxicity at 0.1-mmol and 0.5-mmol concentrations of Omniscan. $^*P < 0.05$ from control. **D**: Effect of Omniscan on cell viability. PBMCs were plated and treated in 96-well plates and incubated for 8 days with various concentrations of Omniscan. Viability of the adherent cells was measured on the eighth day. Data points represent means ± SD of six separate studies. $^*P < 0.05$ compared with control.

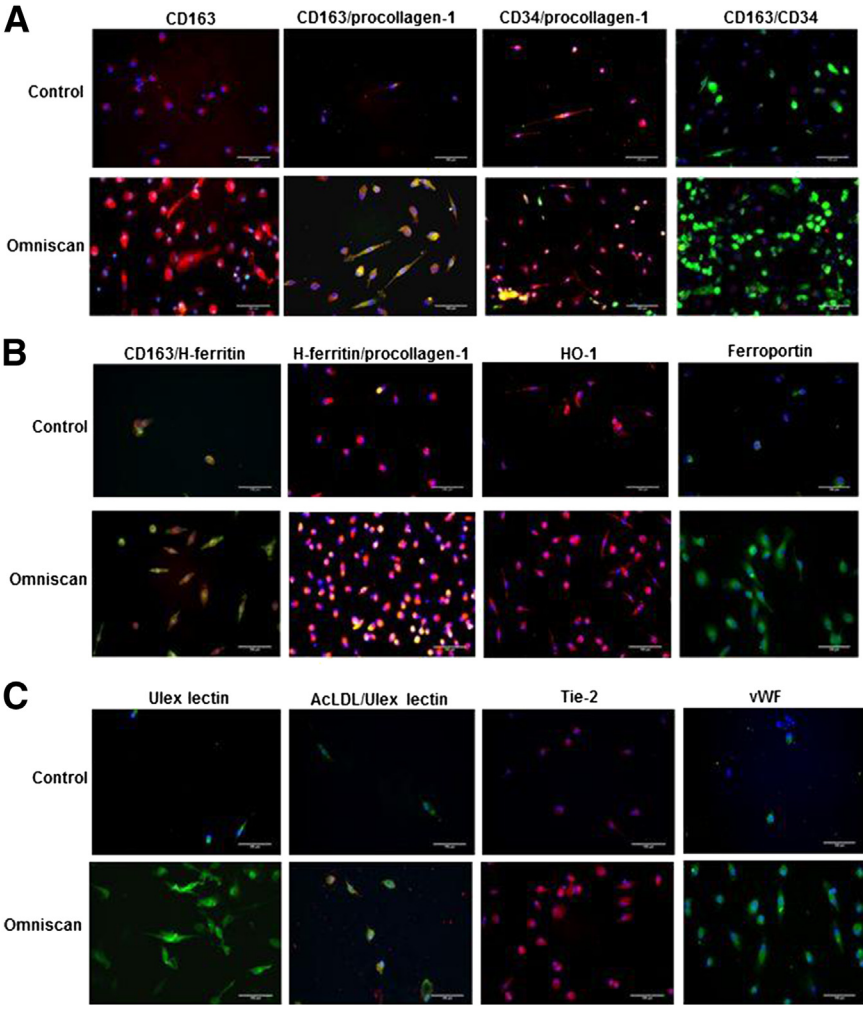

Figure 2 Omniscan-induced cells express procollagen-1, macrophage markers, iron metabolism proteins, and proangiogenic markers as shown by immunofluorescence. **A:** Omniscan-induced, human PBMC—derived adherent cells expressed macrophage marker-CD163 (red) as shown by immunofluorescence. Omniscan-induced cells significantly expressed CD163 (red) and procollagen-1 (green) compared with control cells (double-positive for CD163 and procollagen-1, yellow). The majority of procollagen-1—expressing cells (red) did not express CD34 (green). CD34 was expressed only weakly, and by a small number of $CD163^{+}$ cells (CD34-red and CD163-green). **B:** Omniscan-induced cells express the iron metabolism proteins H-ferritin (green, **top panel**; red, **middle panel**), hemeoxygenase-1 (HO-1) (red), and ferroportin (green). **C:** Compared with control cells, Omniscan-induced cells significantly express the endothelial/pro-angiogenic markers acetylated low-density lipoprotein (AcLDL) (green), Ulex-lectin (red), Tie-2 (red), and von Willebrand factor (VWF) (green). Scale bars: 100 μm. For all immunostaining, appropriate controls included secondary antibody alone and isotype controls (data not shown).

phycoerythrin, FITC, or allophycocynin-labeled IgG isotype control (eBiosciences, Inc./R&D Systems or Santa Cruz Biotechnology, Inc.). Each sample was resuspended in 0.3 mL 1× PBS and analyzed on a FACSCalibur flow cytometer (Becton, Dickinson and Co., Franklin Lakes, NJ). At least 10,000 cells were analyzed per staining. Data were analyzed using CellQuest software (Becton, Dickinson and Co.). Viable cells were identified by gating on forward and side scatters. Data are shown as a logarithmic histogram or dot-plots and expressed as mean fluorescence intensity, obtained from the statistical analysis of the fluorescence height and mean value of the *x* axis displayed by the software. Data were obtained from flow cytometry analyses from six independent experiments.

Quantitative Real-Time PCR

Human PBMCs were cultured with different doses of Omniscan (0.1 and 0.5 mmol). Transcript levels were measured by a two-step, RT-PCR method. Total RNA was extracted from the control and gadolinium contrast—treated adherent cells by RNAqueous-4PCR kit (Ambion, Inc., Austin, TX). DNA synthesis was performed using a Verso cDNA Synthesis kit from Dharmacon RNAi Technology (Thermo Scientific, Pittsburgh, PA). Amplification reaction was performed with a Dharmacon (Thermo Scientific) Solaris real-time quantitative PCR master mix, using 1 μL of cDNA and 1.25 μL of a gene-specific Solaris primers/probe set (CD163, procollagen-1, osteocalcin, Runt-related transcription factor 2). The differential mRNA levels between control and experimental groups were evaluated by the $2^{\Delta\Delta Ct}$ comparative method where ΔCt is the difference between the threshold cycle for target and S3 ribosomal protein or glyceraldehyde-3-phosphate dehydrogenase (ΔCT = Ctx-CtR), and ΔΔCt corresponds to the differences of ΔCt between experimental and control samples (ΔΔCt = ΔCte-ΔCtc).

In Vitro Mineralization Assays

Cultures were seeded in fibronectin-coated chamber slides with 150×10^3 PBMCs or in 6-well culture plates at 5×10^6 cells per well in Dulbecco's modified Eagle's medium supplemented with 10% fetal bovine serum, 2 mmol/L L-glutamine, 100 U/mL penicillin, 100 μg/mL streptomycin, and 0.25 μg/mL amphotericin B, and treated with 0.5 mmol/L Omniscan for 8 days. Media were changed to the complete differentiation medium containing low-glucose DMEM with 15% osteogenic stimulatory supplements, further supplemented

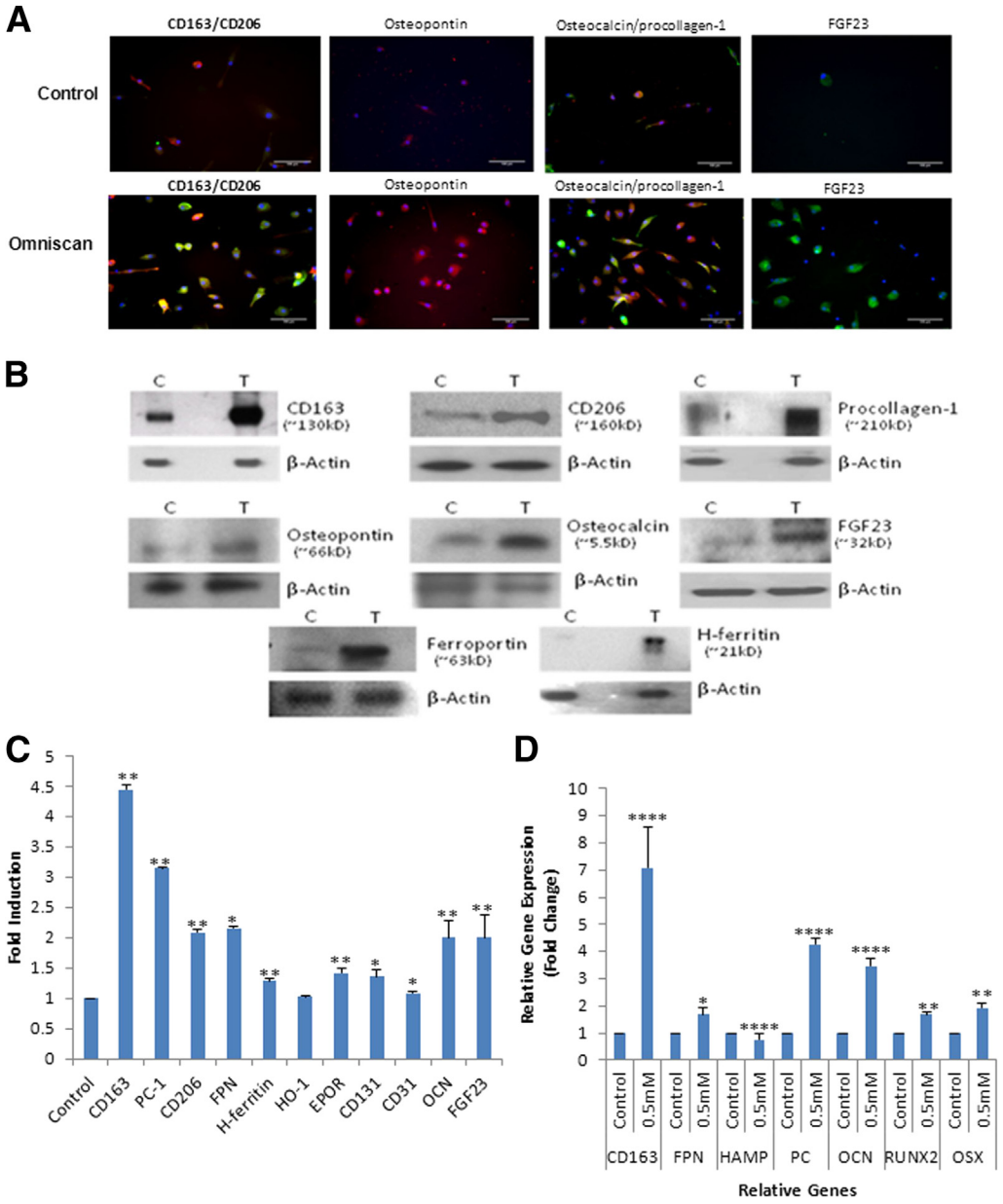

Figure 3 Omniscan-induced cells have an osteogenic phenotype. **A:** Osteoblast-lineage marker expression by PBMCs treated with 0.5 mmol/L Omniscan using immunofluorescence. Omniscan-induced, human PBMC-derived adherent cells express the macrophage markers CD163 (red) and CD206 (green) as shown by immunofluorescence. Omniscan-induced cells significantly expressed osteopontin (red), osteocalcin (red), procollagen-1 (green), and were double-positive for osteocalcin and procollagen-1 (yellow) compared with control cells. The majority of Omniscan-induced cells expressed FGF23 (green). Scale bars: 100 μm. **B:** Protein expression by Omniscan-induced cells. Western blot analysis of human PBMCs treated (T) with 0.5 mmol/L Omniscan or untreated (C) were performed using total cell lysates from adherent cells, as described in *Materials and Methods*. Detection for CD163, CD206, H-ferritin, ferroportin, procollagen-1, osteocalcin (OCN), osteopontin, and FGF23 expression was performed by immunoblotting. The representative blots in the figure show increased expression of these markers by Omniscan-induced cells compared with controls. The same blots were stripped and reprobed with β-actin antibody. **C:** Graphic representation of densitometric scans of Western blots. Data presented were derived from six separate experiments (donors) with or without 0.5 mmol/L Omniscan treatment, and means ± SEM of band intensities in fold induction above control of representative proteins were plotted. On the plot, 1 on the *x* axis represents the controls. $*P < 0.05$, $**P < 0.01$ compared with controls. **D:** Quantitative gene expression by Omniscan-induced cells. cDNA was synthesized from RNA isolated from Omniscan-induced adherent cells. Solaris quantitative real-time PCR gene expression reagents (Dharmacon) were used to detect *CD163*, procollagen-1, ferroportin, hepcidin, Runt-related transcription factor 2 (*Runx2*), Osterix (*OSX, SP7*), and reference genes. cDNA and relative gene expression was calculated from quantification cycle (Cq) values using a delta deltaCq. The figure shows increased gene expression of CD163, ferroportin, procollagen-1, osteocalcin, and osteoblast transcription factors (*Runx-2* and *OSX*) by Omniscan-induced cells compared with controls. $*P < 0.05$, $**P < 0.01$, and $****P < 0.0001$, for Omniscan-treated cells compared with controls.

with a 3.5 mmol/L concentration of β-glycerophosphate, 10^{-8} mol/L dexamethasone, and 50 μg/mL ascorbic acid (Stemcell Technologies, Vancouver, BC, Canada). Cultures were replenished every 3 to 4 days with complete differentiation medium for up to 5 weeks. After 3 and 5 weeks in the differentiation medium, adherent cells were washed twice with 1× PBS and fixed with 4% formaldehyde for 30 minutes, washed two times with distilled water, and stained with 2% alizarin red

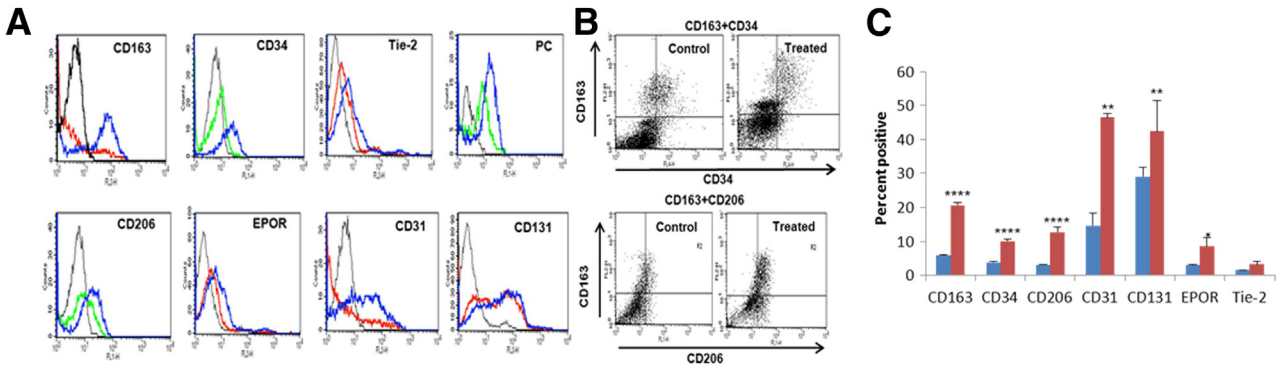

Figure 4 Omniscan-induced cells express macrophage markers, procollagen-1, and proangiogenic markers as shown by flow cytometry analysis. PBMCs were cultured and treated with Omniscan and adherent cells were stained with monoclonal antibodies and then analyzed by flow cytometry. **A:** Histograms show the fluorescence intensity of isotype control antibody (**black line**) compared with untreated (**red line** or **green line**) and Omniscan-treated (**blue line**) cells. The data are presented as means ± SEM ($n = 6$ separate donors). **B:** Representative dot plots show increased CD163, CD34, and CD206 expression by Omniscan-induced cells compared with controls. **C:** A graph shows the cumulative data derived from the six donors and shows the percentage of positive cells present on untreated and Omniscan-induced cells The data are presented as means ± SEM. $*P < 0.05$, $**P < 001$, and $****P < 0.0001$ as compared with controls.

and von Kossa stain (Sigma-Aldrich) to detect any calcified nodules. After staining, cells were washed three times with distilled water. Cells were visualized under a light microscope and images were captured for qualitative or quantitative analysis.

Immunohistochemistry

Ten archived, formalin-fixed, paraffin-embedded skin biopsy specimens diagnosed with NSF were retrieved from the University of Arkansas for Medical Sciences dermatopathology database. We retrieved existing autopsy tissues of patients who died without end-stage kidney disease and NSF to obtain skin, coronary artery, and heart controls. Immunohistochemical staining was performed on newly cut sections for CD34, CD206, CD163, ferroportin, procollagen-1, and osteocalcin. Some sections were double-labeled for CD34/procollagen-1, CD34/CD163, CD163/procollagen-1, and CD206/procollagen-1 using the Envision G|2 Doublestain System (Dako North America, Inc., Carpinteria, CA). Antigen retrieval was performed and the endogenous background activities were blocked.

Approval from the institutional review boards of the University of Arkansas for Medical Sciences and Central Arkansas Veterans Health Care System (Little Rock, AR) were obtained to conduct this study. All clinical investigations were conducted according to Declaration of Helsinki principles. Statistical analyses of the data obtained were performed using SigmaStat from Jandel Scientific (San Rafael, CA). Analysis of the data was performed using an unpaired two-tailed Student's *t*-test. Values are expressed as the arithmetic mean ± 1 SEM. Differences in means with a *P* value less than 0.05 were considered statistically significant.

Results

Omniscan-Induced Cells are Collagen-Secreting CD163/Ferroportin$^+$/Osteocalcin$^+$/FGF23$^+$ Cells

Omniscan (gadodiamide) treatment was not cytotoxic at the concentrations (0.1 or 0.5 mmol) used for the study as shown by a lactate dehydrogenase release assay. However, Omniscan (0.1, 0.5, and 2.5 mmol) induced a dose-dependent differentiation of human PBMCs into significantly more adherent cells than controls as shown by the increased absorbance with CCK-8 assays (Figure 1, C and D). With light microscopy, at 8 days of culture, the number of adherent cells was increased significantly in PBMCs cultured with 0.1 mmol/L (data not shown) and 0.5 mmol/L Omniscan (these concentrations are comparable with serum levels achieved in patients with advanced renal insufficiency exposed to gadolinium contrast[2] than in controls). The morphology of adherent cells varied from spindle to polygonal shape and in some areas they appeared to be in small clusters, suggesting a fusogenic phenotype (Figure 1A).[15] The effect of the iodinated contrast Omnipaque (iohexol) (GE Healthcare, Inc.) on differentiation of PBMCs into adherent cells was similar to controls (Figure 1A). DAPI and Ki-67 staining did not reveal an increase in nuclear division of the Omniscan-treated cells, suggesting that the increase in cell numbers is due to increased cell survival rather than proliferation (Figure 1B).

Omniscan-induced PBMC-derived adherent cells significantly expressed hematopoietic/macrophage markers CD163 and CD206 and the mesenchymal marker procollagen-1 (Figures 2A and 3A). Omnipaque did not induce expression of these markers on adherent cells (data not shown). Dual immunofluorescence showed that many Omniscan-induced CD163$^+$ cells were CD34-negative (Figure 2A). Omniscan-induced CD163$^+$ cells expressed iron metabolism proteins (H-ferritin, hemeoxygenase-1, and ferroportin) (Figure 2B), angiogenic markers (acetylated low-density lipoprotein, Ulex lectin, Tie-2, and von Willebrand factor) (Figure 2C), and osteoblast-lineage markers (osteocalcin, osteopontin, and FGF23) (Figure 3A). Immunofluorescence data were verified with Western blot, which confirmed increased expression of CD163, CD206, ferroportin, H-ferritin, procollagen-1, osteocalcin, osteopontin, and FGF23 by Omniscan-induced cells (Figure 3, B and C). Flow cytometry further confirmed

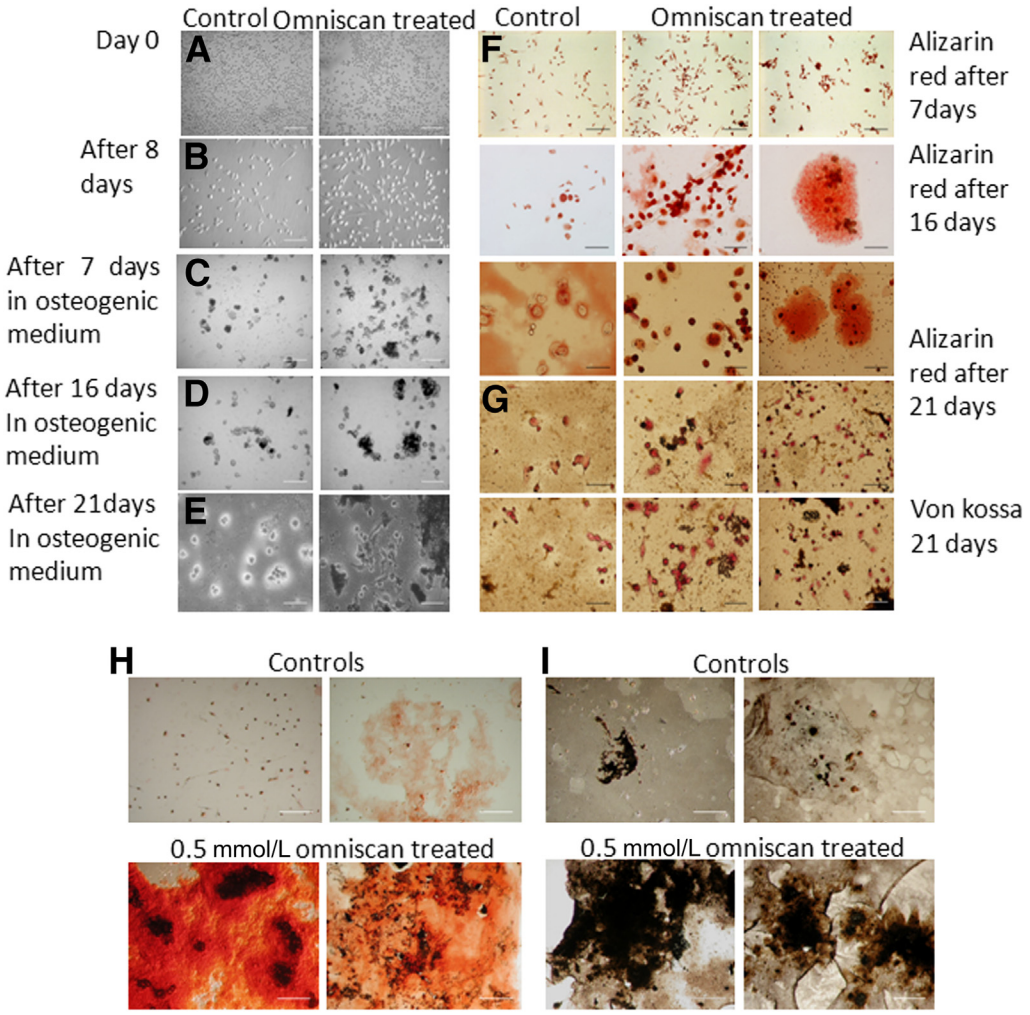

Figure 5 Omniscan-induced cells form mineralized nodules *in vitro*. PBMCs (150×10^3) were plated in fibronectin-coated chamber slides or in 6-well culture plates at 5×10^6 cells per well in Dulbecco's modified Eagle's medium supplemented with 10% fetal bovine serum, 2 mmol/L L-glutamine, 100 U/mL penicillin, 100 μg/mL streptomycin, and 0.25 μg/mL amphotericin B, and treated with a 0.5-mmol/L concentration of Omniscan for 8 days. On day 9 the medium was removed from the wells and replaced with osteogenic differentiation medium with supplements, as mentioned in *Materials and Methods*. Panels show representative light microscopic images. PBMCs on day zero (**A**) and after 8 days of Omniscan treatment (**B**). **C**–**E**: Omniscan-treated cells in osteogenic differentiation medium for different days as indicated. Calcium deposition and mineralized nodules as detected by alizarin red (**F**) and with von Kossa staining (**G**) after 7, 16, and 21 days, and 5 weeks in osteogenic medium. **H**: A high-power view showing significantly increased calcium deposition and mineralized nodule formation (alizarin red staining) by Omniscan-induced cells compared with controls. **I**: A high-power view showing significantly increased calcium deposition and mineralized nodule formation (brownish black by von Kossa staining) by Omniscan-induced cells compared with controls.

that Omniscan-induced $CD163^+$ cells express CD34, CD206, procollagen-1, CD31, CD131, erythropoietin receptor, and Tie-2 (Figure 4).

Omniscan-Induced $CD163^+$ Cells Express Osteoblast Transcription Factors and Have an Osteogenic Phenotype *in Vitro*

Quantitative real-time PCR confirmed the phenotype of Omniscan-induced adherent cells because they expressed significantly more mRNA message for osteoblast transcription factors (osterix and runt-related transcription factor 2), as well as for FGF23, procollagen-1, CD163, and ferroportin, than control cells (Figure 3D). Confirming the functional significance of this finding, Omniscan-induced adherent cells were able to cluster with calcium-phosphate deposition and formed significantly more mineralized nodules under osteogenic conditions as detected by alizarin red and von Kossa staining (Figure 5).

Collagen-Secreting $CD163^+$ $Osteocalcin^+$ Cells Accumulate in Tissues of NSF Patients

To lend support for the pathophysiologic relevance of our *in vitro* findings and to identify cells with an Omniscan-induced phenotype, tissue biopsy specimens or autopsy tissues of 10 NSF patients were examined and analyzed by immunohistochemistry staining. For the control, biopsy specimens from the end-stage renal disease patients without NSF were used. The images to represent specific findings are

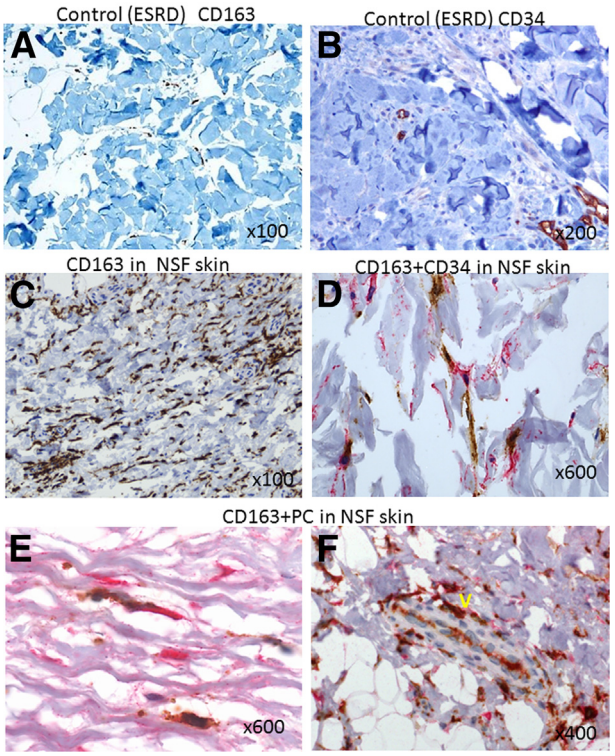

Figure 6 CD163$^+$, CD34, and procollagen$^+$ cells accumulate in the skin of NSF patients. **A:** Only a small number of CD163$^+$ cells (brown) were present in the skin of end-stage renal disease (ESRD) patients with no NSF control. **B:** CD34 staining of ESRD patient (control) skin, showing no staining for CD34-positive cells. **C:** Extensive infiltration of spindled CD163$^+$ macrophages (brown) in the lesional dermis of a patient with NSF. **D:** A CD163$^+$ spindled macrophage (brown) in close juxtaposition with a CD34$^+$ fibrocyte (red) in the dermis of a patient with NSF. In this biopsy specimen, one of the cells was also double positive for CD163 (brown) and CD34 (red). **E:** High-power view showing procollagen-1 (brown) and CD163 (brown) double-positive cells in the dermis of a NSF patient. **F:** A vessel-like (V) structure in the dermis of a NSF patient lined by CD163 (brown) and procollagen-1 (red) double-positive cells. Original magnification, ×100 (**A** and **C**); ×200 (**B**); ×400 (**F**); ×600 (**D** and **E**).

shown in Figures 6, 7, and 8. As shown in Figure 6, skin biopsy specimens of patients without NSF have very few CD163$^+$ cells (Figure 6A) or no CD34$^+$ cells (Figure 6B), whereas in the skin biopsy specimens from NSF patients, numerous dermal and subcutaneous CD163$^+$ cells (Figure 6C) and CD34$^+$ cells (Figure 6D) co-expressing CD163$^+$ were present, and a juxtaposition between CD163$^+$ cells and CD34$^+$ fibrocytes (Figure 6D) was observed. These CD163$^+$ cells were largely spindle-shaped (similar to the morphology observed *in vitro*). By using double immunostaining, we showed that CD163$^+$ cells were positive for procollagen-1, confirming their collagen-secreting phenotype observed *in vitro* (Figure 6E). In the dermis of some NSF biopsy specimens, vessel-like structures lined by CD163$^+$ and procollagen-1–positive cells were present (Figure 6F). CD163$^+$ cells expressed the iron-export protein ferroportin (Figure 7, A and B). Many of these cells also expressed CD206 (data not shown) and were osteocalcin-positive (Figure 7, C and D). NSF patient biopsy specimens also showed the presence of infiltrating CD31$^+$ cells in the dermis (Figure 7E). Our immunohistochemistry results showed that in the NSF patients, CD163$^+$ cells were present not only in the skin but also in other tissues. Figure 8 shows significantly more CD163$^+$ cells in the intima, media, and perivascular tissues of coronary arteries from NSF patients (Figure 8, B and C) than in the coronary artery of an end-stage renal disease patient who did not have NSF (Figure 8A). The same vessel from the NSF patient also showed significant intimal and medial accumulation of osteocalcin (Figure 8C). In a deceased patient with NSF, we observed extensive collagen-secreting CD163$^+$ cell infiltration in the myocardium (Figure 8, D and E). We previously reported the gadolinium (344.4 μg/g and 48.9 μg/g) and iron content (207 μg/g and 354 μg/g) in this patient's aorta and myocardium, respectively.[11] Figure 8F shows co-expression of CD163$^+$ and procollagen$^+$ cells in the lining of a vessel of the periaortic adventitia of an NSF patient. Significantly fewer CD163$^+$ cells were observed in the myocardium of patients who died without having NSF (Figure 8, G and H).

Discussion

In this article, we present the novel observation that Omniscan induces the development of CD163$^+$/ferroportin$^+$

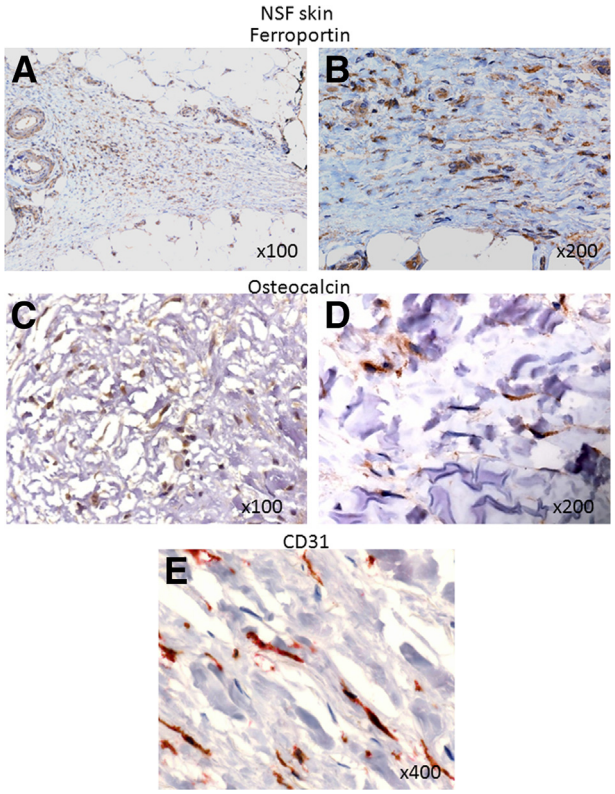

Figure 7 Ferroportin$^+$, osteocalcin$^+$, and CD31$^+$ cell expression in the skin of NSF patients. Extensive infiltration of cells expressing ferroportin (brown) in the lesional dermis and adipose tissue of a patient with NSF. **C** and **D:** Osteocalcin expression (brown) by infiltrating cells in the dermis of NSF patients. **E:** CD31 (red) expression by the infiltrating cells in the dermis of a NSF patient. Original magnification, ×100 (**A** and **C**); ×200 (**B** and **D**); ×400 (**E**).

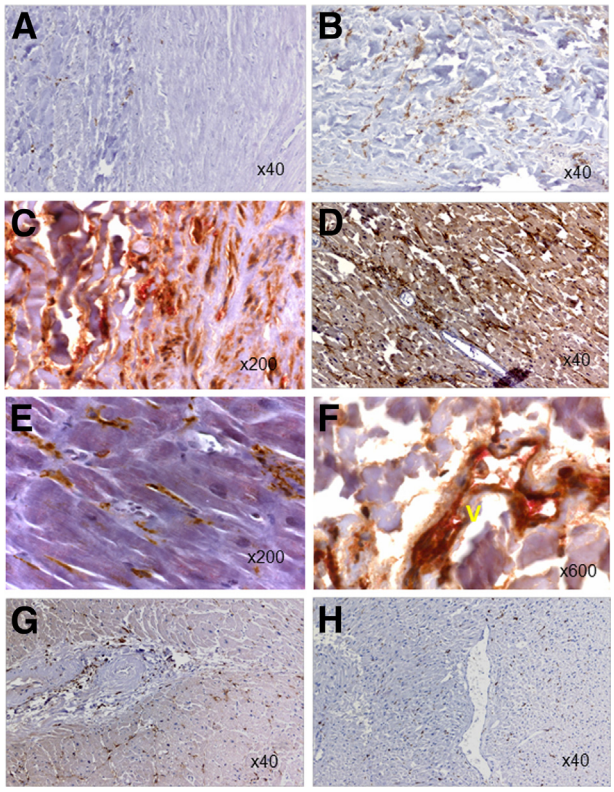

Figure 8 CD163$^+$, procollagen$^+$, and osteocalcin$^+$ cells accumulate in other tissues of NSF patients. **A:** Paucity of CD163$^+$ cells (brown) in the coronary artery of an end-stage renal disease patient without NSF. **B:** Significant CD163$^+$ cells (brown) are present in the coronary artery of this patient who died with NSF. **C:** The presence of CD163 (brown) and procollagen-1 (red) double-positive cells in the aortic media and adventitia of a patient who died with NSF.The aorta showed significant intimal and medial calcification. **D:** Myocardium of a patient who died with NSF shows increased CD163$^+$ cells (brown). **E:** A high-power view confirming increased CD163$^+$ cells (brown) in the myocardium of a patient with NSF. **F:** A lining of a vessel (V) in the periaortic adventitia of a NSF patient lined by CD163 (brown) and procollagen-1 (red) double-positive cells. Note red blood cells in the lumen of the vessel shown. Small numbers of scattered CD163$^+$ cells (brown) in the myocardium of patients with end-stage renal disease (**G**) and end-stage renal disease patients with head and neck cancer (**H**). Original magnification: ×40 (**A**, **B, D, G,** and **H**); ×200 (**C** and **E**); ×600 (**F**).

cells from human PBMCs *in vitro*. These cells express osteogenic markers (runt-related transcription factor 2, osteocalcin, procollagen-1, and FGF23) and angiogenic markers (acetylated low-density lipoprotein, Ulex lectin, Tie-2, CD31, erythropoietin receptor, and von Willebrand factor) and form mineralized nodules under osteogenic conditions *in vitro*. The pathophysiologic relevance of these *in vitro* findings is supported by our demonstration of infiltration of collagen-secreting CD163$^+$/ferroportin$^+$/osteocalcin$^+$ cells in the dermis, subcutaneous adipose tissue, vessel wall, perivascular adventitia, and myocardium of multiple NSF patients, and showing that collagen-secreting CD163$^+$ cells line vessels in NSF patient biopsy specimens.

NSF is characterized by systemic fibrosis and heterotopic ossification in the dermis and other tissues such as of the heart[6–8,16–18] and joints.[8] The cellular mechanisms by which gadolinium could induce systemic fibrosis and ossification are unknown. Circulating Tie-2$^+$ monocyte-derived cells previously have been implicated in heterotopic skeletogenesis/ossification of fibrodysplasia ossificans progressive[19,20] and in bone formation related to fractured healing.[21] Our findings showing expression of osteoblast transcription factors and bone matrix proteins in collagen-secreting Tie-2$^+$/CD163$^+$ cells *in vitro*, and the ability of these cells to form mineralized nodules *in vitro*, suggests an important role of Omniscan-induced cells in heterotopic ossification seen in NSF. This is supported by our demonstration of increased osteogenic cells in NSF patient biopsy specimens. Of importance, we have observed FGF23 expression by osteogenic cells in NSF. This is a novel observation and our findings suggest a potential contribution from tissue osteogenic cells to FGF23 in NSF.[22] FGF23 levels are associated with increased mortality, and FGF23 recently was shown to induce left ventricular hypertrophy.[23,24] High calcium and phosphorus levels have been implicated as risk factors in NSF. It is possible that high endogenous calcium x phosphate product in uremic patients might facilitate the development of osteogenic cells and thus contribute to the pathogenesis of NSF. Our ongoing studies with end-stage kidney disease patients also might clarify some of these mechanisms. It is of interest that sodium thiosulfate, a mineralization inhibitor,[25] has been shown to improve NSF.[26]

Circulating fibrocytes have been suggested to be involved in NSF pathogenesis.[27–29] In a recent study, the addition of Omniscan reduced the ability of the fibrocyte differentiation inhibitor serum amyloid P to decrease fibrocyte differentiation.[28] The collagen-secreting CD163$^+$ osteogenic cells induced by Omniscan may represent unique cells that express hematopoietic, mesenchymal, and endothelial markers simultaneously and with similarities to hemosteoblasts,[30,31] monocyte-derived mesenchymal progenitor cells,[32] early endothelial progenitor cells,[30,31] and fibrocytes.[33–35] Unique features of the Omniscan-induced osteogenic cells include expression of endothelial markers (such as von Willebrand factor), iron metabolism proteins, and erythropoietin receptors, which are not known to be expressed by fibrocytes.[32,36] The experimental conditions used in our study may be important in optimally identifying the unique effects of Omniscan on PBMCs. We chose *in vitro* concentrations of gadolinium in our experiments based on previous observations of *in vivo* concentrations of gadolinium present in end-stage kidney disease patients who received Omniscan. As noted by Joffe et al,[37] elimination t1/2 of administered gadolinium is prolonged to 34 hours in hemodialysis patients and only 66% of the administered gadolinium contrast is eliminated by 21 days in peritoneal dialysis patients. After a 0.1-mmol/kg intravenous dose, serum concentrations of gadolinium were 500 μmol/L in the first few hours to 200 to 250 μmol/L at 24 to 48 hours after injection. In peritoneal dialysis patients, serum gadolinium levels followed a similar trend.

We have previously demonstrated that gadolinium contrast induces iron mobilization in patients who develop NSF.[2] Further, we have demonstrated that iron accumulates in the tissues of NSF patients.[11] Iron is important in the function of prolyl-4-hydroxylase and collagen synthesis and has been implicated in fibrosing disorders.[38,39] Iron is known to increase FGF23 levels.[40,41] The source of iron in NSF remains unknown. The CD163 pathway is important in iron metabolism and iron is exported out of the cell by ferroportin.[42] Our finding demonstrates that the induction of CD163 and ferroportin-expressing cells by gadolinium contrast and significant infiltration of $CD163^+$ $ferroportin^+$ cells in NSF suggests a role for these cells in the iron mobilization and accumulation observed in NSF.

Perivascular and myocardial infiltration of collagen-secreting $CD163^+$ cells in NSF is potentially important in NSF outcome. Perivascular tissue may be exposed to some of the highest concentrations of gadolinium chelate administered through intravascular routes. Thus, perivascular cells (known to express CD163)[43] and tissues may bear the maximum consequences of gadolinium chelate and, consequently, result in the preferential infiltration of $CD163^+$ cells in perivascular tissues. This is supported by recent observations that gadolinium and iron accumulate in large vessels[11] and perivascular tissues in NSF,[44] the finding of perivascular infiltrates[45] and perivascular fibrosis[46] in NSF tissues, and by our previous observation that gadolinium accumulates in human calcific uremic arteriolopathy[5] and our current observation showing vascular, perivascular, and myocardial accumulation of collagen-secreting $CD163^+$ cells. Collectively, these findings could explain the cardiac fibrosis, vascular calcification, and increased cardiac events such as arrhythmias and death seen in NSF.[11]

Although our experiments provide a novel mechanism of Omniscan toxicity, future studies will be required to investigate if the intact gadolinium chelate itself (gadolinium–diethylenetriamine penta-acetic acid bismethylamide plus excess calcium–diethylenetriamine penta-acetic acid bismethylamide) or the gadolinium ion dissociated from the chelate induces the osteogenic cells. Gadolinium is known to activate metabotropic glutamate receptors and glutamate signaling regulates osteoblastic function.[47] Also, the mechanisms of persistence of the clinical phenotype of NSF years after gadolinium contrast exposure would indicate the potential role of uremia-associated factors (such as hyperphosphatemia) or its therapies in sustaining the osteogenic cells, and would merit further investigation.[48] Expression of erythropoietin receptors by Omniscan-induced cells is particularly intriguing because erythropoietin has been suspected to be a co-factor in NSF[49–51] and is known to upregulate ferroportin expression,[52] stimulate endothelial progenitor cell proliferation,[53] and induce osteogenesis.[54]

We present a novel mechanism of gadolinium toxicity potentially mediated through collagen-secreting $CD163^+$ $ferroportin^+$ cells with an osteogenic potential. The findings from our study could explain the cellular basis of major observations seen in NSF, namely systemic fibrosis, heterotopic ossification, iron accumulation, and increased cardiovascular mortality. Future studies are required to further examine the role of these cells in NSF and other systemic fibrosing and calcifying conditions.

Acknowledgments

We thank Dr. Judit Megyesi for assistance with immunofluorescence microscopy and Cindy Reid for technical editing assistance.

References

1. Grobner T: Gadolinium—a specific trigger for the development of nephrogenic fibrosing dermopathy and nephrogenic systemic fibrosis? Nephrol Dial Transplant 2006, 21:1104–1108
2. Swaminathan S, Horn TD, Pellowski D, Abul-Ezz S, Bornhorst JA, Viswamitra S, Shah SV: Nephrogenic systemic fibrosis, gadolinium, and iron mobilization. N Engl J Med 2007, 357:720–722
3. Cowper SE, Su LD, Bhawan J, Robin HS, LeBoit PE: Nephrogenic fibrosing dermopathy. Am J Dermatopathol 2001, 23:383–393
4. Swartz RD, Crofford LJ, Phan SH, Ike RW, Su LD: Nephrogenic fibrosing dermopathy: a novel cutaneous fibrosing disorder in patients with renal failure. Am J Med 2003, 114:563–572
5. Amuluru L, High W, Hiatt KM, Ranville J, Shah SV, Malik B, Swaminathan S: Metal deposition in calcific uremic arteriolopathy. J Am Acad Dermatol 2009, 61:73–79
6. Deng A, Bilu Martin D, Spillane A, Chwalek J, Surin-Lord S, Brooks S, Patrali J, Sina B, Gaspari A, Kao G: Nephrogenic systemic fibrosis with a spectrum of clinical and histopathological presentation: a disorder of aberrant dermal remodeling. J Cutan Pathol 2009, 37:204–210
7. Nagai Y, Hasegawa M, Shinmi K, Kishi C, Tsushima Y, Endo K, Okabe K, Suzuki K, Ishikawa O: Nephrogenic systemic fibrosis with multiple calcification and osseous metaplasia. Acta Derm Venereol 2008, 88:597–600
8. Weigle JP, Broome DR: Nephrogenic systemic fibrosis: chronic imaging findings and review of the medical literature. Skeletal Radiol 2008, 37:457–464
9. Quatresooz P, Paquet P, Hermanns-Lê T, Piérard GE: Immunohistochemical aspects of the fibrogenic pathway in nephrogenic systemic fibrosis. Appl Immunohistochem Mol Morphol 2010, 18:448–452
10. Girardi M, Kay J, Elston DM, Leboit PE, Abu-Alfa A, Cowper SE: Nephrogenic systemic fibrosis: clinicopathological definition and workup recommendations. J Am Acad Dermatol 2011, 65:1095–1106
11. Swaminathan S, High WA, Ranville J, Horn TD, Hiatt K, Thomas M, Brown HH, Shah SV: Cardiac and vascular metal deposition with high mortality in nephrogenic systemic fibrosis. Kidney Int 2008, 73:1413–1418
12. Corna G, Campana L, Pignatti E, Castiglioni A, Tagliafico E, Bosurgi L, Campanella A, Brunelli S, Manfredi AA, Apostoli P, Silvestri L, Camaschella C, Rovere-Querini P: Polarization dictates iron handling by inflammatory and alternatively activated macrophages. Haematologica 2010, 95:1814–1822
13. Gössl M, Mödder UI, Atkinson EJ, Lerman A, Khosla S: Osteocalcin expression by circulating endothelial progenitor cells in patients with coronary atherosclerosis. J Am Coll Cardiol 2008, 52:1314–1325
14. Broome DR: Nephrogenic systemic fibrosis associated with gadolinium based contrast agents: a summary of the medical literature reporting. Eur J Radiol 2008, 66:230–234

15. Helming L, Gordon S: Macrophage fusion induced by IL-4 alternative activation is a multistage process involving multiple target molecules. Eur J Immunol 2007, 37:33–42
16. Koreishi AF, Nazarian RM, Saenz AJ, Klepeis VE, McDonald AG, Farris AB, Colvin RB, Duncan LM, Mandal RV, Kay J: Nephrogenic systemic fibrosis: a pathologic study of autopsy cases. Arch Pathol Lab Med 2009, 133:1943–1948
17. Ruiz-Genao DP, Pascual-Lopez MP, Fraga S, Aragues M, Garcia-Diez A: Osseous metaplasia in the setting of nephrogenic fibrosing dermopathy. J Cutan Pathol 2005, 32:172–175
18. Hershko K, Hull C, Ettefagh L, Nedorost S, Dyson S, Horn T, Gilliam AC: A variant of nephrogenic fibrosing dermopathy with osteoclast-like giant cells: a syndrome of dysregulated matrix remodeling? J Cutan Pathol 2004, 31:262–265
19. Suda RK, Billings PC, Egan KP, Kim JH, McCarrick-Walmsley R, Glaser DL, Porter DL, Shore EM, Pignolo RJ: Circulating osteogenic precursor cells in heterotopic bone formation. Stem Cells 2009, 27: 2209–2219
20. Lounev VY, Ramachandran R, Wosczyna MN, Yamamoto M, Maidment ADA, Shore EM, Glaser DL, Goldhamer DJ, Kaplan FS: Identification of progenitor cells that contribute to heterotopic skeletogenesis. J Bone Joint Surg Am 2009, 91: 652–663
21. Eghbali-Fatourechi GZ, Lamsam J, Fraser D, Nagel D, Riggs BL, Khosla S: Circulating osteoblast-lineage cells in humans. N Engl J Med 2005, 352:1959–1966
22. Fretellier N, Idee JM, Guerret S, Hollenbeck C, Hartmann D, Gonzalez W, Robic C, Port M, Corot C: Clinical, biological, and skin histopathologic effects of ionic macrocyclic and nonionic linear gadolinium chelates in a rat model of nephrogenic systemic fibrosis. Invest Radiol 2011, 46:85–93
23. Isakova T, Wahl P, Vargas GS, Gutierrez OM, Scialla J, Xie H, Appleby D, Nessel L, Bellovich K, Chen J, Hamm L, Gadegbeku C, Howritz E, Townsend RR, Anderson CA, Lash JP, Hsu CY, Leonard MB, Wolf M: Fibroblast growth factor 23 is elevated before parathyroid hormone and phosphate in chronic kidney disease. Kidney Int 2011, 79:1370–1378
24. Faul C, Amaral AP, Oskouei B, Hu MC, Sloan A, Isakova T, Gutierrez OM, Aguillon-Prada R, Lincold J, Hare JM, Mundel P, Morales A, Scialla J, Fischer M, Soliman EZ, Chen J, Go AS, Rosas SE, Nessel L, Townsend RR, Feldman HI, St John Sutton M, Ojo A, Gadegbeku C, Di Marco GS, Reuter S, Kentrup D, Tiemann K, Brand M, Hill JA, Moe OW, Kuro OM, Kusek JW, Keane MG, Wolf M: FGF23 induces left ventricular hypertrophy. J Clin Invest 2011, 121:4393–4408
25. Hayden MR, Goldsmith DJ: Sodium thiosulfate: new hope for the treatment of calciphylaxis. Semin Dial 2010, 23:258–262
26. Yerram P, Saab G, Karuparthi PR, Hayden MR, Khanna R: Nephrogenic systemic fibrosis: a mysterious disease in patients with renal failure–role of gadolinium-based contrast media in causation and the beneficial effect of intravenous sodium thiosulfate. Clin J Am Soc Nephrol 2007, 2:258–263
27. Cowper SE: Nephrogenic fibrosing dermopathy: the first 6 years. Curr Opin Rheumatol 2003, 15:785–790
28. Vakil V, Sung JJ, Piecychna M, Crawford JR, Kuo P, Abu-Alfa AK, Cowper SE, Bucala R, Gomer RH: Gadolinium-containing magnetic resonance image contrast agent promotes fibrocyte differentiation. J Magn Reson Imaging 2009, 30:1284–1288
29. Quan TE, Cowper SE, Bucala R: The role of circulating fibrocytes in fibrosis. Curr Rheumatol Rep 2006, 8:145–150
30. Rehman J, Li J, Orschell CM, March KL: Peripheral blood "endothelial progenitor cells" are derived from monocyte/macrophages and secrete angiogenic growth factors. Circulation 2003, 107: 1164–1169
31. Romagnani P, Annunziato F, Liotta F, Lazzeri E, Mazzinghi B, Frosali F, Cosmi L, Maggi L, Lasagni L, Scheffold A, Kruger M, Dimmeler S, Marra F, Gensini G, Maggi E, Romagnani S: CD14+CD34 low cells with stem cell phenotypic and functional features are the major source of circulating endothelial progenitors. Circ Res 2005, 97:314–322
32. Cesselli D, Beltrami AP, Rigo S, Bergamin N, D'Aurizio F, Verardo R, Piazza S, Klaric E, Fanin R, Tofoletto B, Marzinotto S, Mariuzzi L, Finato N, Pandolfi M, Leri A, Schneider C, Beltrami CA, Anversa P: Multipotent progenitor cells are present in human peripheral blood. Circ Res 2009, 104:1225–1234
33. Abe R, Donnelly SC, Peng T, Bucala R, Metz CN: Peripheral blood fibrocytes: differentiation pathway and migration to wound sites. J Immunol 2001, 166:7556–7562
34. Chesney J, Bucala R: Peripheral blood fibrocytes: mesenchymal precursor cells and the pathogenesis of fibrosis. Curr Rheumatol Rep 2000, 2:501–505
35. Mathai SK, Gulati M, Peng X, Russell TR, Shaw AC, Rubinowitz AN, Murray LA, Siner JM, Antin-Ozerkis DE, Montgomery RR, Reilkoff RAS, Bucala RJ, Herzog EL: Circulating monocytes from systemic sclerosis patients with interstitial lung disease show an enhanced profibrotic phenotype. Lab Invest 2010, 90:812–823
36. Tintut Y, Demer L: The hemosteoblast: friend or foe? Circ Res 2011, 108:1038–1039
37. Joffe P, Thomsen HS, Meusel M: Pharmacokinetics of gadodiamide injection in patients with severe renal insufficiency and patients undergoing hemodialysis or continuous ambulatory peritoneal dialysis. Acta Radiol 1998, 5:491–502
38. Guzman NA, Ascari WQ, Cutroneo KR, Desnick RJ: Comparison between avian and human prolyl 4-hydroxylases: studies on the holomeric enzymes and their constituent subunits. J Cell Biochem 1992, 48:172–189
39. Otogawa K, Ogawa T, Shiga R, Nakatani K, Ikeda K, Nakajima Y, Kawada N: Attenuation of acute and chronic liver injury in rats by iron-deficient diet. Am J Physiol Regul Integr Comp Physiol 2008, 294:R311–R320
40. Takeda Y, Komaba H, Goto S, Fujii H, Umezu M, Hasegawa H, Fujimori A, Nishioka M, Nishi S, Fukagawa M: Effect of intravenous saccharated ferric oxide on serum FGF23 and mineral metabolism in hemodialysis patients. Am J Nephrol 2011, 33: 421–426
41. Shimizu Y, Tada Y, Yamauchi M, Okamoto T, Suzuki H, Ito N, Fukumoto S, Sugimoto T, Fujita: Hypophosphatemia induced by intravenous administration of saccharated ferric oxide: another form of FGF23-related hypophosphatemia. Bone 2009, 45: 814–816
42. Vallelian F, Schaer CA, Kaempfer T, Gehrig P, Duerst E, Schoedon G, Schaer DJ: Glucocorticoid treatment skews human monocyte differentiation into a hemoglobin-clearance phenotype with enhanced heme-iron recycling and antioxidant capacity. Blood 2010, 116:5347–5356
43. Kim WK, Alvarez X, Fisher J, Bronfin B, Westmoreland S, McLaurin J, Williams K: CD163 identifies perivascular macrophages in normal and viral encephalitic brains and potential precursors to perivascular macrophages in blood. Am J Pathol 2006, 168: 822–834
44. Schroeder JA, Weingart C, Coras B, Hausser I, Reinhold S, Mack M, Seybold V, Vogt T, Banas B, Hofstaedter F, Kramer BK: Ultrastructural evidence of dermal gadolinium deposits in a patient with nephrogenic systemic fibrosis and end-stage renal disease. Clin J Am Soc Nephrol 2008, 3:968–975
45. Kroshinsky D, Kay J, Nazarian RM: Case records of the Massachusetts General Hospital. Case 37-2009. A 46-year-old woman with chronic renal failure, leg swelling, and skin changes. N Engl J Med 2009, 361:2166–2176
46. Mendoza FA, Artlett CM, Sandorfi N, Latinis K, Piera-Velasquez S, Jimenez SA: Description of 12 cases of nephrogenic fibrosing dermopathy and review of the literature. Semin Arthritis Rheum 2006, 35:238–249

47. Taylor AF: Osteoblastic glutamate receptor function regulates bone formation and resorption. J Musculoskelet Neuronal Interact 2002, 2: 285−290
48. Fretellier N, Idée JM, Bruneval P, Guerret S, Daubiné F, Jestin G, Factor C, Poveda N, Dencausse A, Massicot F, Laprévote O, Mandet C, Bouzian N, Port M, Corot C: Hyperphosphataemia sensitizes renally impaired rats to the profibrotic effects of gadodiamide. Br J Pharmacol 2010, 165:1151−1162
49. Swaminathan S, Ahmed I, McCarthy JT, Albright RC, Pittelkow MR, Caplice NM, Griffin MD, Leung N: Nephrogenic fibrosing dermopathy and high-dose erythropoietin therapy. Ann Intern Med 2006, 145:234−235
50. Swaminathan S, Shah SV: New insights into nephrogenic systemic fibrosis. J Am Soc Nephrol 2007, 18:2636−2643
51. Hope TA, High WA, LeBoit PE, Chaopathomkul B, Rogut VS, Herfkens RJ, Brasch RC: Nephrogenic systemic fibrosis in rats treated with erythropoietin and intravenous iron. Radiology 2009, 253:390−398
52. Robach P, Recalcati S, Girelli D, Gelfi C, Aachmann-Andersen NJ, Thomsen JJ, Norgaard AM, Alberghini A, Campostrini N, Castagna A, Vigana A, Santambrogio P, Kempf T, Wollert KC, Moutereau SP, Lundby C, Cairo G: Alterations of systemic and muscle iron metabolism in human subjects treated with low-dose recombinant erythropoietin. Blood 2009, 113:6707−6715
53. Bahlmann FH, de Groot K, Spandau J-M, Landry AL, Hertel B, Duckert T, Boehm SM, Menne J, Haller H, Floser D: Erythropoietin regulates endothelial progenitor cells. Blood 2004, 103: 921−926
54. Shiozawa Y, Jung Y, Ziegler AM, Pedersen EA, Wang J, Wang Z, Song J, Wang J, Lee CH, Sud S, Pienta KJ, Krebsbach PH, Taichman RS: Erythropoietin couples hematopoiesis with bone formation. PLoS One 2010, 5:e10853